AALBORG UNIVERSITY
DENMARK

# MAS Based Event-Triggered Hybrid Control for Smart Microgrids

Dou, Chunxia; Liu, Bin; Guerrero, Josep M.

# MAS Based Event-Triggered Hybrid Control for Smart Microgrids

Chunxia Dou[*],    Bin Liu,    Josep M. Guerrero, *Senior Member IEEE*

*Abstract*—**This paper is focused on an advanced control for autonomous microgrids. In order to improve the performance regarding security and stability, a hierarchical decentralized coordinated control scheme is proposed based on multi-agents structure. Moreover, corresponding to the multi-mode and the hybrid characteristics of microgrids, an event-triggered hybrid control, including three kinds of switching controls, is designed to intelligently reconstruct operation mode when the security stability assessment indexes or the constraint conditions are violated. The validity of proposed control scheme is demonstrated by means of simulation results.**

*Index terms*—**Microgrid, multi-agents, hybrid control, event-triggered**

## I. Introduction

THE increased penetration of Distributed Energy Sources (DERs) in recent power network introduced the new concept Microgrid (MG) [1]. MGs have received increasing attention as an effective way of integrating DERs into the electricity network, which is formed generally by confined cluster of loads, storage devices, and small generators, also named microsources. The MG has the ability as single entity to work in both grid-connected and islanded modes of operation [2,3]. A MG needs smart control strategies in order to use renewable energy resources to meet the demand of energy with high reliability, flexibility and cost effectiveness. Hence, the smart MG is being observed by many governments as a way to locally solve global energetic problems.

Compared with a traditional power system, the smart MG is facing more challenges w.r.t. the following aspects:
*1) More complex system;* a MG contains many kinds of DERs like Distributed Generation Units (DGUs) and distributed storage devices, which have different dynamic characteristics [4,5]. *2) More complex hybrid dynamic behavior;* many DGUs have both continuous and discrete dynamic behaviors. Their generating electricity characteristics comply with physical laws and display continuous dynamic behavior. Simultaneously, they generally operate in multiple modes subjected to natural condition changes, which are described as event-driven discrete behavior. Moreover, these hybrid behaviors interact with each other [6]. *3) More uncertainties of operation;* in a MG, there exist many DGUs whose power outputs are highly dependent on natural conditions. Such a renewable energy resource often offers an intermittent and uncertain power supply. *4) Multi-mode operation;* in a MG, DGUs have to operate in multiple modes subjected to natural condition changes, which is accompanied by frequent switching mode between the discharging and charging states of store units [7,8].

With respect to the above challenges, when designing a smart MG, it is necessary to consider the following factors:
*1) Corresponding to the multi-mode feature of MG, a smart MG should be designed as a Multiple Agent System (MAS) to realize the real-time reconfiguration of operation mode.*

MAS is an autonomous system, in which many agent are grouped together and depend on each other via cooperation and competition to form a community to achieve the goals of individuals and the whole MAS [9,10]. Owing to its desirable properties related to *autonomy, reactivity as well as social ability and pro-activeness*, MAS may handle some complex problems more flexibly and efficiently[11,12]. Therefore, the control based on MAS may be able to reconstruct the operational mode and network configuration of MG in a flexible manner so that MG can meet the demand on variable energy with high reliability, flexibility and effective cost even in uncertain operational environment.
*2) Corresponding to the conspicuous hybrid behaviors, a smart MG can be designed as a hybrid control consisting of continuous control, discrete control and interaction each other.*

In order to effectively control the hybrid dynamic behavior, a smart MG is required to handle not only a local high-level continuous controller to regulate dynamic behaviors, but also an on-line logic coordinated control to manage discrete behavior. It is most important that the smart control is needed to implement real-time interaction between discrete and continuous controls, which means that the smart control is typical hybrid control [13-15].

By the factors given above, in this paper, we propose a hybrid control scheme based on MAS for smart MG in order to

*Chun-xia Dou is with Institute of Electrical Engineering, Yanshan University, Qinhuangdao 066004, China.
(e-mail: cxdou@ysu.edu.cn)
Bin Liu is currently with School of Electrical & Information Engineering, The University of Sydney, NSW 2006, Australia, and with Department of Information and Computation Sciences, Hunan University of Technology, Zhuzhou 412008, China.
(e-mail: bin.liu@sydney.edu.au)
Josep M. Guerrero is with Department of Energy Technology, Aalborg University, 9220 Aalborg East, Denmark
(e-mail:joz@et.aau.dk)

improve stability and security performance.

In this paper, we start the control scheme by building a model based on MAS by using Differential Hybrid Petri-net (DHPN). Then, an event-triggered hybrid control is proposed, including three kinds of switching controls: (1) internal switching control for operation mode according to the constraint conditions of local continuous state variable, (2) global coordinated switching control for operation mode based on Security Stability Assessment Indexes (SSAIs), and (3) switching control for continuous dynamics followed by the change of operation mode. The event-triggered hybrid control, which is implemented by using the enabling and junction functions associated with test arcs, normal arcs and inhibitor arcs in the DHPN, can intelligently reconstruct operation mode of MG in a flexible and adaptive manner according to operational states.

The paper is organized as follows. The hybrid model is presented in Section II. In Section III, the event-triggered hybrid control is analysed. The simulation examples are provided to demonstrate the effectiveness of the proposed hybrid control in Section IV. Concluding remarks are summarized in Section V.

## II. MAS Based Hybrid Model of MG

In island mode, some units may arrange on the frequency and voltage of the MG by means of the local primary control, namely droop control, e.g. frequency and control droops [16-18]. Therefore, the intelligent reconfigure strategies are required to switch operational mode of DERs so as to meet load demand on different situation and maintain secure performance [19]. Corresponding to different architecture of MG, the reconfigure strategies of operational mode should also be different. In this paper, an example of autonomous MG is shown in Fig.1, which contains a renewable photovoltaic energy generation, a renewable wind energy generation, a fuel cell and microturbine power generation set, a battery system and a group of loads. Here, management and control of each generation unit are carried out by their respective agents, and the coordinated control of operational modes is implemented on the upper level coordinated control agent.
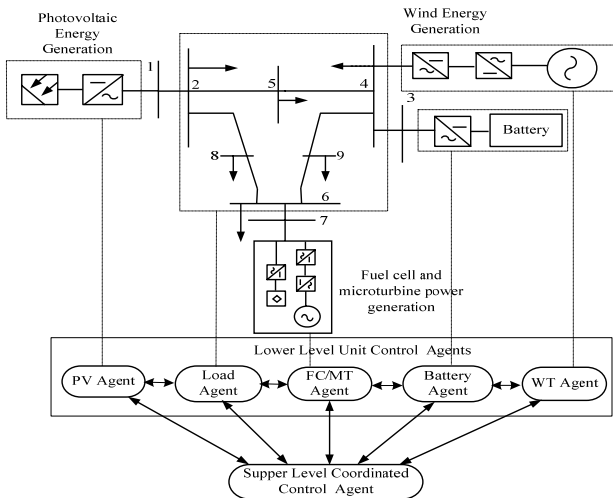


Fig.1. Multi-agent structure of an autonomous MG

In this paper, a MAS based DHPN model is built to de-

scribe hybrid behaviors of the MG. A DHPN can be defined by a 14-tuple ($P_D$, $T_D$, $P_{DF}$, $T_{DF}$, $X$, $A_N$, $A_I$, $A_T$, $P_{re}$, $P_{os}$, $\Gamma$, $H$, $J$, $M_0$) [20-22].

Corresponding to the six agents as shown in Fig.1, the MG model is described by six DHPN models respectively as shown in Fig. 2, including one coordinated control DHPN model and five unit control DHPN models. In every DHPN model, discrete places represent the operation modes of its agent, differential place describes its continuous states, differential transitions represent its continuous dynamics, and discrete transitions are defined as the occurrence of the discrete events that result in switch of operation mode. More detailed descriptions regarding the places and the transitions are given in Tables 1-4.
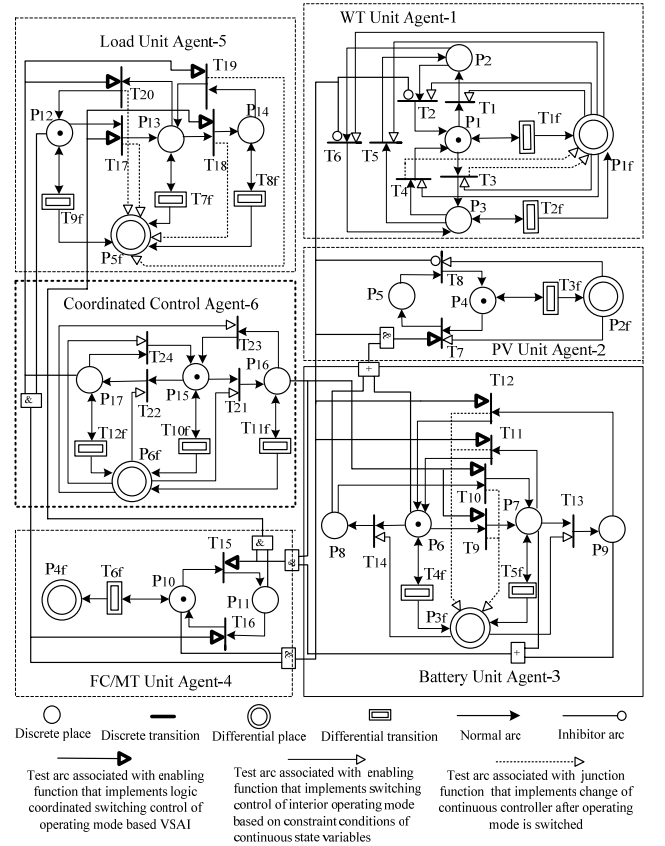


Fig.2. DHPN model of multi-agent MG

TABLE 1. Description Of Discrete Places In The DHPN Model

| Discrete Places | Description |
|---|---|
| $P_1$ | Maximum Power Point Tracking (MPPT) operation mode in Wind Turbine (WT) unit agent |
| $P_2$ | Stopping operation mode in WT unit agent |
| $P_3$ | Constant power output operation mode in WT unit agent |
| $P_4$ | MPPT operation mode in Photovoltaic (PV) unit agent |
| $P_5$ | Stopping operation mode in PV unit agent |
| $P_6$ | Charging operation mode in battery unit agent |
| $P_7$ | Discharging operation mode in battery unit agent |
| $P_8$ | Stopping operation mode with maximal State of Charge (SOC) in battery |
| $P_9$ | Stopping operation mode with minimal SOC in battery |
| $P_{10}$ | Low power output mode in Fuel Cell/Microturbine (FC/MT) unit agent |
| $P_{11}$ | Rated power output mode in FC/MT unit agent |
| $P_{12}$ | Full load operation mode in load unit agent |

| | |
|---|---|
| P13 | Part load operation mode in load unit agent |
| P14 | light load operation mode in load unit agent |
| P15 | Normal voltage operation mode in MG |
| P16 | Insecure low voltage operation mode in MG |
| P17 | Insecure high voltage operation mode in MG |

TABLE 2. DESCRIPTION OF DISCRETE TRANSITIONS IN THE DHPN MODEL

| Discrete Transitions | Description |
|---|---|
| T1 | WT switches to stopping mode from MPPT mode |
| T2 | WT switches to MPPT mode from stopping mode |
| T3 | WT switches to constant output mode from MPPT mode |
| T4 | WT switches to MPPT mode from constant output mode |
| T5 | WT switches to stopping mode from constant output mode |
| T6 | WT switches to constant output mode from stopping mode |
| T7 | PV switches to stopping mode from MPPT mode |
| T8 | PV switches to MPPT mode from stopping mode |
| T9 | Battery switches to discharging mode from charging mode |
| T10 | Battery switches to discharging mode from stopping mode with maximal SOC |
| T11 | Battery switches to charging mode from discharging mode |
| T12 | Battery switches to charging mode from stopping mode with minimal SOC |
| T13 | Battery stops discharging because SOC reaches to minimal value |
| T14 | Battery stops charging because SOC reaches to maximal value |
| T15 | FC/MT switches to rated mode from low output mode |
| T16 | FC/MT switches to low output mode from rated mode |
| T17 | Part load shedding |
| T18 | maximal load shedding |
| T19 | Load partly restored |
| T20 | Load fully restored |
| T21 | SSAI is lower than minimal secure value |
| T22 | SSAI is higher than maximal secure value |
| T23 | SSAI rises to normal range |
| T24 | SSAI drops to normal range |

Here, all discrete transitions are defined as "logically true", That is, a discrete transition is triggered when its connected enabling function is activated. At the moment, only if its pre-place has token, its corresponding event must occur, known as "transition fires".

TABLE 3. DESCRIPTION OF DIFFERENTIAL PLACES IN THE DHPN MODEL

| Differential Places | Description |
|---|---|
| P1f | Continuous states in WT unit agent |
| P2f | Continuous states in PV unit agent |
| P3f | Continuous states in battery unit agent |
| P4f | Continuous states in FC/MT unit agent |
| P5f | Continuous states in load unit agent |
| P6f | Main node voltage states in MG |

TABLE 4. DESCRIPTION OF DIFFERENTIAL TRANSITIONS IN THE DHPN MODEL

| Differential Transitions | Description |
|---|---|
| T1f andT2f | Continuous dynamics of WT corresponding to P1 and P3 operating modes respectively |
| T3f | Continuous dynamics of PV on P4 operating mode |
| T4f and T5f | Continuous dynamics of battery corresponding to P6 and P7 operating modes respectively |
| T6f | Continuous dynamics of FC/MT on P10 operating mode |
| T7f-- T9f | Continuous dynamics of load corresponding to P13, P14 and P12 operating modes respectively |
| T10f-- T12f | Real-timely assessing dynamic voltages of MG corresponding to P15---P17 operating modes respectively |

Here, all differential transitions $T_{1f} - T_{9f}$ are described by the differential equation $\dot{\mathbf{x}}_i = f_{is}(\mathbf{x}_i, \mathbf{u}_{is}, t)$, where, $i$ represents the $i$-th agent, and $s$ is the $s$-th mode of the $i$-th agent. The differential transitions $T_{10f} - T_{12f}$ represent real-timely assessing dynamic voltages of the MG.

Normal arc functions $P_{reD}(P_i, T_j)$, $P_{reDDF}(P_i, T_{jf})$, $P_{osD}(P_i, T_j)$ and $P_{osDDF}(P_i, T_{jf})$ are defined as "1". In addition, the normal arc functions $P_{osDFF}(P_{if}, T_{jf})$ is denoted as continuous state vector of respective agent.

Since each agent only runs in one mode, the place corresponding to the operation mode is marked with a token, while the other places have not token. Therefore, there is only one token in each agent DHPN model. In the DHPN model, corresponding to the initial modes of six agents, the initial marking $m_{D10}(P_i)=[1,0,0]$, $m_{D20}(P_i)=[1,0]$, $m_{D30}(P_i)=[1,0,0,0]$, $m_{D40}(P_i)=[1,0]$, $m_{D50}(P_i)=[1,0,0]$, $m_{D60}(P_i)=[1,0,0]$; $m_{F10-F60}(P_{if})$ are the initial state vectors $\mathbf{x}_{i0}$ of the six agents respectively.

By the above description regarding places, transitions and normal arcs, the DHPN model shows only hybrid dynamic behavior of MG, but no hybrid control action is taken. In this paper, the event-triggered hybrid control based on MAS is proposed including three kinds of switching controls: (1) internal switching control for operation mode according to the constraint conditions of local continuous state variables, (2) global coordinated switching control for operation mode based on SSAIs, and (3) switching control for continuous dynamics followed by the change of operation mode. In the designed DHPN model, these hybrid control actions are implemented by enabling functions and junction functions associated with test arcs, as well normal and inhibitor arcs. More details regarding the hybrid control are given in the following sections.

## III.   MAS BASED HYBRID CONTROL

### A.   Switching Control for the Internal Operating Mode of Agents

In the DHPN model, $H_{DF}(P_{if}, T_j)$ is an enabling function associated with a test arc that connects a differential pre-place to a discrete transition. The switching control between operation modes according to the constraints of the continuous state variable, is implemented by means of the enabling function $H_{DF}(P_{if}, T_j)$. The switching control has the following features: (1) is a discrete control driven by continuous state variables, (2) is triggered to switch operation mode when the constraint conditions of the continuous state are violated, and (3) executes internal mode switching in every agent based on its local continuous states. In Fig. 2, the switching controls via $H_{DF}(P_{if}, T_j)$ are defined as follows

$$H_{DF}(P_{1f}, T_1) \xrightarrow{\downarrow} v \le v_{ci} \Rightarrow P_w = 0 ; \quad (1)$$

$$H_{DF}(P_{1f}, T_2) \xrightarrow{\uparrow} v_{ci} < v \le v_R \Rightarrow P_w = P_R(v - v_{ci})/(v_R - v_{ci}) ; \quad (2)$$

$$H_{DF}(P_{1f}, T_3) \xrightarrow{\uparrow} v_R < v \le v_{co} \Rightarrow P_w = P_R ; \quad (3)$$

$$H_{DF}(P_{1f}, T_5) \xrightarrow{\uparrow} v > v_{co} \Rightarrow P_w = 0 ; \quad (4)$$

$$H_{DF}(P_{1f}, T_6) \xrightarrow{\downarrow} v_R < v \le v_{co} \Rightarrow P_w = P_R ; \quad (5)$$

$$H_{DF}(P_{1f}, T_4) \xrightarrow{\downarrow} v_{ci} < v \le v_R \Rightarrow P_w = P_R(v - v_{ci})/(v_R - v_{ci}) ; (6)$$

Where $P_R$ is the rated power of the wind turbine; $v_{ci}$ is the cut-in wind speed; $v_{co}$ is the cut-off wind speed; $v_{ci} < v_R < v_{co}$ is the rated wind speed; "$\downarrow$" represents that

the wind speed drops, and "↑" represents that the wind speed rises. The following descriptions are in the same manner.

$$\text{H}_{DF} \; (\text{P}_{2f},\text{T}_7) \xrightarrow{\downarrow} G_{ing} \le C \Rightarrow P_{PV} = 0 \; ; \qquad (7)$$

$$\text{H}_{DF} (\text{P}_{2f},\text{T}_8) \xrightarrow{\uparrow} G_{ing} > C \Rightarrow P_{PV} = P_{stc}\frac{G_{ing}}{G_{stc}}\left(1+k(T_c - T_r)\right); \qquad (8)$$

where $P_{PV}$ is the PV output power at irradiance $G_{ing}$ ; $P_{stc}$ is the maximum power at the standard condition; $G_{ing}$ is the incident irradiance; $G_{stc}$ is the standard irradiance of $1000\text{W}/m^2$ ; $k$ is the temperature coefficient of power; $T_c$ is the cell temperature; $T_r$ is the reference temperature $25\,^{\circ}\text{C}$, and $C$ is the threshold $G_{ing}$ value, according to the performance of the PV cell.

$$\text{H}_{DF} (\text{P}_{3f},\text{T}_{13}) \xrightarrow{\downarrow} \text{SOC=SOC}_{min} \Rightarrow P_- = 0 \; ; \qquad (9)$$

$$\text{H}_{DF} \; (\text{P}_{3f},\text{T}_{14}) \xrightarrow{\uparrow} \text{SOC=SOC}_{max} \Rightarrow P_+ = 0 \; ; \qquad (10)$$

where $P_+$ and $P_-$ are the charge and the discharge power of battery respectively; $\text{SOC}_{max}$ and $\text{SOC}_{min}$ are the maximum and the minimum state of charge (SOC).

$$\text{H}_{DF} \; (\text{P}_{6f},\text{T}_{21}) \xrightarrow{\downarrow} m(U) \le \text{U}_{min}; \qquad (11)$$

$$\text{H}_{DF} \; (\text{P}_{6f},\text{T}_{22}) \xrightarrow{\uparrow} m(U) > \text{U}_{max}; \qquad (12)$$

$$\text{H}_{DF} (\text{P}_{6f},\text{T}_{23}) \xrightarrow{\uparrow} \text{U}_{min} < m(U) \le \text{U}_e; \qquad (13)$$

$$\text{H}_{DF} \; (\text{P}_{6f},\text{T}_{24}) \xrightarrow{\downarrow} \text{U}_e < m(U) \le \text{U}_{max}; \qquad (14)$$

where $m(U)$ is the voltage stability assessment index (VSAI); $\text{U}_{min}$ is the minimal secure threshold value of voltage; $\text{U}_e$ is the rated voltage; $\text{U}_{max}$ is the maximal secure threshold value of voltage. The VSAI is determined by assessing the voltages in many nodes.

The descriptions of the switching control via enabling function $\text{H}_{DF} (\text{P}_{if},\text{T}_j)$ are given in Table 5.

TABLE 5. DESIGNS OF ENABLING FUNCTIONS REGARDING LOCAL SWITCHING CONTROL OF OPERATING MODE

| Functions | Description |
|---|---|
| $\text{H}_{DF}$ (P1f,T1) | When the continuous state variable drops to $v \le v_{ci}$, the enabling function $\text{H}_{DF}$ (P1f,T1) is activated so that discrete transition T1 is triggered and the operation mode of WT agent is switched to P2 so that $P_w = 0$. |
| $\text{H}_{DF}$ (P1f,T2) | When the continuous state variable rises to $v_{ci} < v \le v_R$, the enabling function $\text{H}_{DF}$ (P1f,T2) is activated so that discrete transition T2 is triggered and the operation mode of WT agent is switched to P1 so that $P_w = P_R(v-v_{ci})/(v_R - v_{ci})$. |
| $\text{H}_{DF}$ (P1f,T3) | When the continuous state variable rises to $v_R < v \le v_{co}$, the enabling function $\text{H}_{DF}$ (P1f,T3) is activated so that discrete transition T3 is triggered and the operation mode of WT agent is switched to P3 so that $P_w = P_R$. |
| $\text{H}_{DF}$ (P1f,T5) | When the continuous state variable rises to $v > v_{co}$, the enabling function $\text{H}_{DF}$ (P1f,T5) is activated so that discrete transition T5 is triggered and the operation mode of WT agent is switched to P2 so that $P_w = 0$. |
| $\text{H}_{DF}$ (P1f,T6) | When the continuous state variable drops to $v_R < v \le v_{co}$, the enabling function $\text{H}_{DF}$ (P1f,T6) is activated so that discrete transition T6 is triggered and the operation mode of WT agent is switched to P3 so that $P_w = P_R$. |
| $\text{H}_{DF}$ | When the continuous state variable drops to $v_{ci} < v \le v_R$, the |

(P1f,T4) enabling function $\text{H}_{DF}$ (P1f,T4) is activated so that discrete transition T4 is triggered and the operation mode of WT agent is switched to P1 so that $P_w = P_R(v-v_{ci})/(v_R - v_{ci})$.

| $\text{H}_{DF}$ (P2f,T7) | When the continuous state variable drops to $G_{ing} \le C$, the enabling function $\text{H}_{DF}$ (P2f,T7) is activated so that discrete transition T7 is triggered and the operation mode of PV agent is switched to P5 so that $P_{PV} = 0$. |
|---|---|
| $\text{H}_{DF}$ (P2f,T8) | When the continuous state variable rises to $G_{ing} > C$, the enabling function $\text{H}_{DF}$ (P2f,T8) is activated so that discrete transition T8 is triggered and the operation mode of PV agent is switched to P4 so that $P_{PV} = P_{stc}\frac{G_{ing}}{G_{stc}}\left(1+k(T_c - T_r)\right)$. |
| $\text{H}_{DF}$ (P3f,T13) | When the continuous state variable drops to SOC=SOCmin, the enabling function $\text{H}_{DF}$ (P3f,T13) is activated so that discrete transition T13 is triggered and the operation mode of battery agent is switched to P9 so that $P_- = 0$. |
| $\text{H}_{DF}$ (P3f,T14) | When the continuous state variable rises to SOC=SOCmax, the enabling function $\text{H}_{DF}$ (P3f,T14) is activated so that discrete transition T14 is triggered and the operation mode of battery agent is switched to P8 so that $P_+ = 0$. |
| $\text{H}_{DF}$ (P6f,T21) | When the continuous voltage assessment index drops to $m(U) \le \text{U}_{min}$, the enabling function $\text{H}_{DF}$ (P6f,T21) is activated so that discrete transition T21 is triggered and the operation mode of coordinated agent is switched to P16. |
| $\text{H}_{DF}$ (P6f,T23) | When the continuous voltage assessment index rises to $\text{U}_{min} < m(U) \le \text{U}_e$, the enabling function $\text{H}_{DF}$ (P6f,T23) is activated so that T23 is triggered and the operation mode of coordinated agent is switched to P15. |
| $\text{H}_{DF}$ (P6f,T22) | When the continuous voltage assessment index rises to $m(U) > \text{U}_{max}$, the enabling function $\text{H}_{DF}$ (P6f,T22) is activated so that T22 is triggered and the operation mode of coordinated agent is switched to P17. |
| $\text{H}_{DF}$ (P6f,T24) | When the continuous voltage assessment index drops to $\text{U}_e < m(U) \le \text{U}_{max}$, the enabling function $\text{H}_{DF}$ (P6f,T24) is activated so that T24 is triggered and the operation mode of coordinated agent is switched to P15. |

### B. Coordinated Switching Control for Operating Modes Among Agents

In the DHPN model, $\text{H}_D (\text{P}_i,\text{T}_j)$ is an enabling function associated with a normal arc that connects a discrete pre-place to a discrete transition. The coordinated switching control of operation mode is designed via the enabling function $\text{H}_D (\text{P}_i,\text{T}_j)$. The switching control presents the following features: (1) it is a discrete control driven mainly by the voltage operation mode of whole MG associated with the operation modes of other unit agents, (2) it is triggered to switch operation mode when voltage is assessed insecure based on the VSAI, and (3) it implements the coordinated switching mode among agents. In addition, the inhibitor function $\text{P}_{reDI}(\text{P}_i, \text{T}_j)$ is designed to restrict the switching mode under certain conditions. In order to establish the coordinated control, logic relation ships between the operation modes among unit agents are set by using logic circuits as follows

$$\overline{\text{P}} = \text{P}_{16} (\text{P}_7 + \text{P}_9); \quad \overline{\overline{\text{P}}} = \text{P}_{11} \text{P}_{16} (\text{P}_7 + \text{P}_9); \quad \widetilde{\text{P}} = \text{P}_{12} \text{P}_{17};$$

$$\widetilde{\widetilde{\text{P}}} = \text{P}_{10} \text{P}_{12} \text{P}_{17}; \quad \hat{\text{P}} = \text{P}_{10} \text{P}_{12} \text{P}_{17}(\text{P}_6 + \text{P}_8).$$

Due to the aforementioned, the design of the coordinated switching control via the enabling function $\text{H}_D(\text{P}_i,\text{T}_j)$ and the inhibitor $\text{P}_{reDI}(\text{P}_i, \text{T}_j)$, is described in Tables 6 and 7.

TABLE 7. DESIGNS OF ENABLING FUNCTIONS REGARDING COORDINATED CONTROL AMONG DHPN MODELS

| Functions | Description |
|---|---|
| $H_D$ $(P_{16},T_9)$ | When the discrete pre-place $P_{16}$ has token, the enabling function is activated so that discrete transition $T_9$ is triggered. In this case, only if the pre-place $P_6$ has token, the operation mode of battery will be switched to $P_7$, otherwise, mode does not change. |
| $H_D$ $(P_{16},T_{10})$ | When the discrete pre-place $P_{16}$ has token, the discrete transition $T_{10}$ is also triggered. In this case, only if the pre-place $P_8$ has token, the operation mode of battery will be switched to $P_7$. |
| $H_D$ $(\overline{P},T_{15})$ | When the place $P_{16}$ and anyone of $P_7$ and $P_9$ have tokens simultaneously, the discrete transition $T_{15}$ is triggered. In this case, only if the pre-place $P_{10}$ has token, the operation mode of FC/MT will be switched to $P_{11}$. |
| $H_D$ $(\overline{\overline{P}},T_{17})$ | When the places $P_{11}$, $P_{16}$ and anyone of $P_7$ and $P_9$ have tokens simultaneously, the discrete transition $T_{17}$ is triggered. In this case, only if the pre-place $P_{12}$ has token, the operation mode of load will be switched to $P_{13}$. |
| $H_D$ $(\overline{\overline{P}},T_{18})$ | When the places $P_{11}$, $P_{16}$ and anyone of $P_7$ and $P_9$ have tokens simultaneously, the discrete transition $T_{18}$ is also triggered. In this case, only if the pre-place $P_{13}$ has token, the operation mode of load will be switched to $P_{14}$. |
| $H_D$ $(P_{17},T_{19})$ | When the discrete pre-place $P_{17}$ has token, the discrete transition $T_{19}$ is triggered. In this case, only if the pre-place $P_{14}$ has token, the operation mode of load will be switched to $P_{13}$. |
| $H_D$ $(P_{17},T_{20})$ | When the discrete pre-place $P_{17}$ has token, the discrete transition $T_{20}$ is also triggered. In this case, only if the pre-place $P_{13}$ has token, the operation mode of load will be switched to $P_{12}$. |
| $H_D$ $(\widetilde{P},T_{16})$ | When the places $P_{12}$ and $P_{17}$ have tokens simultaneously, the discrete transition $T_{16}$ is triggered. In this case, only if the pre-place $P_{11}$ has token, the operation mode of FC/MT will be switched to $P_{10}$. |
| $H_D$ $(\widetilde{\widetilde{P}},T_{11})$ | When the places $P_{10}$, $P_{12}$ and $P_{17}$ have tokens simultaneously, the discrete transition $T_{11}$ is triggered. In this case, only if the pre-place $P_7$ has token, the operation mode of battery will be switched to $P_6$. |
| $H_D$ $(\hat{P},T_{12})$ | When the places $P_{10}$, $P_{12}$, $P_{17}$ and anyone of $P_6$ and $P_8$ have tokens simultaneously, the discrete transition $T_{12}$ is triggered. In this case, only if the pre-place $P_4$ has token, the operation mode of PV will be switched to $P_5$. |

TABLE 7. DESIGNS OF INHIBITOR FUNCTIONS REGARDING COORDINATED CONTROL AMONG DHPN MODELS

| Functions | Description |
|---|---|
| $Pre_{DI}$ $(\widetilde{\widetilde{P}},T_2)$ | The discrete transition $T_2$ is restricted not triggering when the places $P_{10}$, $P_{12}$ and $P_{17}$ have token simultaneously. |
| $Pre_{DI}$ $(\widetilde{\widetilde{P}},T_6)$ | The discrete transition $T_6$ is restricted not triggering when the places $P_{10}$, $P_{12}$ and $P_{17}$ have token simultaneously. |
| $Pre_{DI}$ $(\widetilde{\widetilde{P}},T_8)$ | The discrete transition $T_2$ is restricted not triggering when the places $P_{10}$, $P_{12}$ and $P_{17}$ have marking simultaneously. |

## C. Switching Control for the Continuous Dynamics of Agents

In the DHPN model, $J(T_j, P_i)$ is a junction function associated with a test arc that connects a discrete transition to a differential post-place. The switching control of continuous dynamics followed by the change of the operation mode is designed by using the junction function. The switching control presents the following features: (1) it is discrete control driven by discrete event, (2) it is triggered to switch the controller of continuous dynamics when the corresponding operation mode changes, and (3) it implements the switching of the continuous controller in every agent for the stability purposes. In Fig. 2, the design of the switching control via the junction function $J(T_j, P_i)$ is described in Table 8.

TABLE 8. DESIGNS OF JUNCTION FUNCTIONS REGARDING LOCAL SWITCHING CONTROL OF CONTINUOUS DYNAMICS

| Functions | Description |
|---|---|
| $J(T_3,P_{1f})$ | When the discrete transition $T_3$ fires, the continuous controller for $P_{1f}$ dynamics is switched to the constant power regulating mode from the MPPT regulating mode. |
| $J(T_4,P_{1f})$ | When the discrete transition $T_4$ fires, the continuous controller for $P_{1f}$ dynamics is switched to the MPPT regulating mode from the constant power regulating mode. |
| $J(T_9,P_{3f})$ $J(T_{10},P_{3f})$ | When the discrete transition $T_9$ or $T_{10}$ fires, the continuous controller for $P_{3f}$ dynamics is switched to the discharging dynamic regulating mode from the charging regulating mode. |
| $J(T_{11},P_{3f})$ $J(T_{12},P_{3f})$ | When the discrete transition $T_{11}$ or $T_{12}$ fires, the continuous controller for $P_{3f}$ dynamics is switched to the charging dynamic regulating mode from the discharging regulating mode. |
| $J$ $(T_{17},P_{5f})$ | When the discrete transition $T_{17}$ fires, the continuous controller for $P_{5f}$ dynamics is switched to the part load shedding dynamic regulating mode from the full load regulating mode. |
| $J$ $(T_{18},P_{5f})$ | When the discrete transition $T_{18}$ fires, the continuous controller for $P_{5f}$ dynamics is switched to the light load dynamic regulating mode from the part load regulating mode. |
| $J$ $(T_{19},P_{5f})$ | When the discrete transition $T_{19}$ fires, the continuous controller for $P_{5f}$ dynamics is switched to the part load dynamic regulating mode from the light load regulating mode. |
| $J$ $(T_{20},P_{5f})$ | When the discrete transition $T_{20}$ fires, the continuous controller for $P_{5f}$ dynamics is switched to the part load dynamic regulating mode from the full load regulating mode. |

## IV. SIMULATION RESULTS

In order to test the performance of the proposed control approach, the MG shown in Fig.1 has been simulated under load following performance.

Four distributed generation unit agents supply power to the loads, as shown in Fig. 3(a). The load following performance under the proposed hybrid control is shown in Fig. 3(b) and (c).
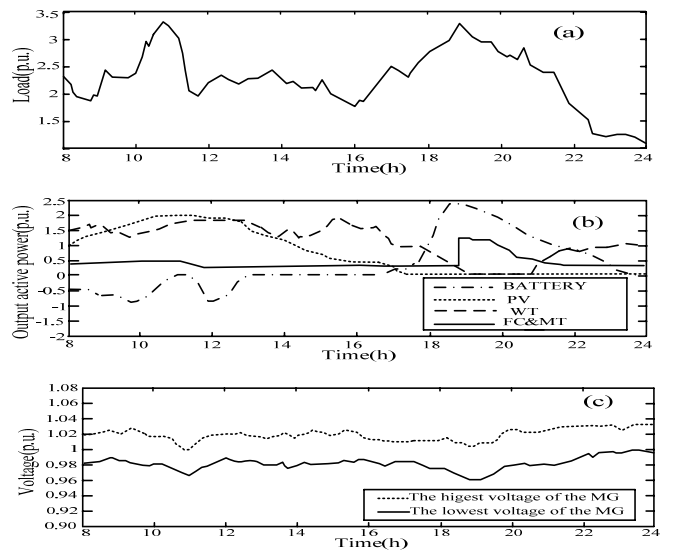


Fig.3 Load following performance

Fig. 3(a) is the load curve from 8.00h to 24.00h during a day. And Fig. 3(b) shows the optimal active power outputs of four distributed generation unit agents. From Fig. 3(b), it can be seen that the PV unit agent operates in MPPT mode as long as possible. Only after 17.00h, due to solar energy de-

creases to bellow the threshed value, the PV unit agent has to stop the operation. Along the simulation, subjected to the wind speed, the WT unit agent operates in three modes: form 11.00h to 13.00h, the WT unit operates in constant output power mode since the wind speed is higher than the higher threshed value; form 17.00h to 18.45h, in stopping operation mode since the wind speed is lower than the lower threshed value; the rest of time, in MPPT mode. On the other hand, during most of the time, the FC/MT unit agent operates in low power output mode to reduce the cost as much as possible. Only during 19.00h to 20.25h, subjected to natural conditions (sunshine and wind), both renewable energy PV and WT units stop generating electricity, but in order to meet larger load demand, the FC/MT unit agent has to switch to the rated operation mode. Since the battery unit agent acts as master source implementing a grid-forming control, when renewable energy generated electricity is higher than the load demand, the battery unit runs in charging operation mode. However, when renewable energy generating electricity is lower than the load demand, the battery unit operates in discharging operation mode. In the particular case that the renewable energy generated electricity exactly meets the load demand, the battery unit stops running. Therefore, the battery unit agent frequently switches between three operation modes in order to match unbalanced powers. Fig.3(c) displays the highest and lowest voltage levels of the autonomous MG. Fig.3(c) shows that during all the time, the voltage is controlled between 0.94p.u. and 1.04p.u., and the fluctuation value is limited in the range of ±4 percentage of rating value. This is due to the fact that the hybrid control can maintain better voltages while following the load profile.

## V. CONCLUSION

In this paper, an event-triggered hybrid control based on MAS has been proposed for smart MGs. The smart reconfiguration strategies between operation modes have been implemented by three kinds of event-triggered hybrid controls via DHPN for improving the security and stability performance. Simulation results show that the proposed hybrid control can maintain security and stability performance better by real-timely switching operational mode while following the load profile.

## REFERENCES

[1] N. Hatziargyriou, H. Asano, et al, "Microgrids," IEEE Power & Energy Magazine, vol.6, pp.78-94, 2007.

[2] R. H. Lasseter, "Microgrids," Power Engineering Society Winter Meeting, New York, UAS, 2002.

[3] IEEE Std.1547.4-2007, "Island systems with electric power systems," 2007.

[4] A. R. Yasser, E. S. F. Ehab, "Adaptive decentralized droop controller to preserve power sharing stability of paralleled inverters in distributed generation microgrids," IEEE Transactions on Power Electronics, vol.23, pp. 2806-2816, 2008.

[5] E. Barklund, N. Pogaku, M. Prodanovic, C. H. Aramburo, T. C. Green, "Energy management in autonomous microgrid using stability –constrained droop control of inverter," IEEE Transactions on Power Electronics, vol.25, pp.2346-2352, 2008.

[6] Z. H. Jiang, L. J. Gao, R. A. Dougal, "Flexible multiobjective control of power converter in active hybrid fuel cell/ battery power sources," IEEE Tran. Power Electr,vol.20, pp.245-254, 2005.

[7] Z. H. Jiang, L..J. Gao, R. A. Dougal, "Adaptive control strategy for active power sharing in hybrid fuel cell/battery power sources," IEEE Tran.

Energy Conver, vol.22, pp.183-194, 2007.

[8] D. B. Nelson, M. N. Nehrir, C. Wang, "Unit sizing and cost analysis of stand-alone hybrid wind/PV/ fuel cell power generation system," Renewable Energy, vol.31, pp.1641-1656, 2006.

[9] S. D. J. Mcarthur, E. M. Davidson, V. M. Catterson, et al, "Multiagent systems for power engineering applications, Part I: Concepts, approaches, and technical challenges," IEEE Transactions on Power Systems, vol.22, pp.1743-1752, 2007.

[10] C. C. Liu, "Agent modeling for integrated power systems," Final Project Report, Power Systems Engineering Research Center, PSERC, September, 2008.

[11] A. L. Dimeas, N. D. Hatziargyrious, "Agent based control for Microgrids," IEEE PES General Meeting, Tampa, FL, June, 2007.

[12] A. L. Dimeas, N. D. Hatziargyrious, "Operation of a multiagent system for microgrid control," IEEE Transactions on Power Systems, vol.20, pp.1447-1455, 2005.

[13] C. X. Dou, B. Liu, "Hierarchical hybrid control for improving comprehensive performance in smart power system," International Journal of Electrical Power & Energy Systems, vol.43, pp.595-606, 2012.

[14] C. X. Dou, B. Liu, "Transient control for microgrid with multiple distributed generations based on hybrid system theory," International Journal of Electrical Power & Energy Systems, vol.42, pp.408-417, 2012.

[15] C. X. Dou, D. L. Liu, X. B. Jia, F. Zhao, "Management and control for smart microgrid based on hybrid control theory," Electric Power Component and System, vol.39, pp.813-32, 2011.

[16] K. D. Brabandere, B. Bolsens, "A Voltage and Frequency Droop Control Method for Parallel Inverters," IEEE Transactions on Power Electronics, vol.22, pp.2501-2507, 2007.

[17] T. L. Vandoorn, J. D. M. De Kooning, B. Meersman, Josep M. Guerrero, L. Vandevelde, "Voltage-based control of a smart transformer in a Microgrid,"IEEE Transactions on Industrial Electronics, vol.60, pp. 1291-1305, 2013.

[18] M. Savaghebi, A. Jalilian, J. C. Vasquez, Josep M. Guerrero, "Autonomous voltage unbalance compensation in an islanded droop-controlled Microgrid,", IEEE Transactions on Industrial Electronics, vol.60, pp. 1390-1402, 2013.

[19] Josep M. Guerrero, P. C. Loh, M. Chandorkar, T. L. Lee, "Advanced control architectures for intelligent Microgrids – Part I: decentralized and hierarchical control," IEEE Transactions on Industrial Electronics, vol.60, pp. 1254-1262, 2012.

[20] V. K. Paruchuri, A. Davari, A. Feliachi, "Hybrid modeling of power system using hybrid Petri net," In Proc. Southeastern Symposium on System Theory, pp.221-224, 2005.

[21] N. Lu, J. H. Chow, A. A. Desrochers, "A multi-layer Petri net model for deregulated electric power systems," In Proc. Amer. Contr. Conf., Anchorage, AK, pp. 513-518, 2002.

[22] J. Sun, S. Y. Qin, Y. H. Song, "Fault diagnosis of electric power systems based on fuzzy Petri nets," IEEE Transactions on Power System, vol.19, pp.2053-2059, 2004.